IEEE Access
Multidisciplinary | Rapid Review | Open Access Journal

Received December 18, 2019, accepted March 16, 2020, date of publication March 26, 2020, date of current version April 13, 2020.

Digital Object Identifier 10.1109/ACCESS.2020.2983619

Runway Width Design Based on Wheel Trace Distribution Test

DUOYAO ZHANG, XINGANG SHI, LIANGCAI CAI, GUANHU WANG, CHAOMEI MENG, AND LEI LIANG

Department of Airport Construction Engineering, Air Force Engineering University, Xi'an 86710038, China

Corresponding author: Xingang Shi (kgdwxsxg@163.com)

This work was supported by the National Natural Science Foundation of China under Grant No.: 51578540 (Study on the plane distribution of cumulative fatigue of cement concrete pavement in military airport) and Grant No.: 51608526 (Study on damage mechanism of cement concrete pavement under complex mechanical behavior of new aircraft).

ABSTRACT The current runway width design in China was still according to the aircraft size and the accumulated experience in the flight process, and there is no clear calculation method. This paper proposed a new runway width design method based on the wheel traces distribution of the aircraft. A laser test system was developed to measure the aircraft wheel tracks of 17 cross sections along the runway at a feeder airport. The test results indicated that when aircraft takes off or lands, the transverse wheels traces obeyed a normal distribution. The variation curve in landing was selected to fit a numerical formula, which was used to calculate the maximum landing variation within the forward motion range, and the expression of the wheel trace transverse distribution on the section with the maximum discretization was determined. At last, a failure probability of 0.0001% was chosen as the criterion to determine the runway width. It was showed that B737-30 should have at least 45 m width to ensure the 0.0001 % failure probability.

INDEX TERMS Runway width design, wheel trace transverse distribution, site test, change rule.

I. INTRODUCTION

Runway width design is an important part of airport planning, which is the key linkage to ensure the aircraft safely running on the runway, instead of veering off [1]. Currently, the runway width was mainly based on the transverse distribution statistics and determined by calculating the safe running probability. In early 21st century, the US Federal Aviation Administration, cooperated with Airbus and Boeing, carried out systematic testing and research for the wheel trace transverse distributions of B747 and A380 aircraft. The risk factors [2]–[5] of B747 airplanes on runways with different widths were calculated by the method of extreme value analysis. In the international airport design standards given by ICAO and adopted by US, Australia, and the Netherlands, etc., it is accepted that the wheel trace transverse distribution is modelled well by a Gaussian type distribution. Moreover, the mean and reference variation are presented through tests, and the corresponding runway widths were calculated [6]–[8]. The tests for wheel trace transverse distributions of different military and civilian aircrafts were also conducted in China. Li and Wang *et al* had recorded the wheel tracks of various military aircrafts, and all of them drawn the conclusion that the wheel tracks obey the normal distribution [9], [10]. Chinese specifications for asphalt pavement design of civil airports (MH/T 5010-2017) [11] was also based on the normal distribution of lateral traffic volume. Li [12] studied the course stability and lateral stability of aircraft during takeoff and landing and deduced a theoretical calculation formula for lateral offset. Cen *et al.* [13] proposed a method to caculate runway width based on the reliability principle using the wheel lateral distribution test results in the touchdown zone.

It can be seen from above investigations that the wheel trace transverse distributions during aircraft takeoff and landing processes were the predominant factor to determine the runway width. Although the researchers from China and abroad had used various methods to measure the wheel traces of different aircrafts [14]–[16], some researchers still considered that the research on aircraft wheel trace transverse distribution had imperfections. As the aircraft passes different runway cross sections, the wheel trace transverse distribution changes accordingly. However, there is limited information in the literature that describes the above issue and usually selected only one or several sections to carry out the tests. The partial runway selection cannot guarantee the selected

The associate editor coordinating the review of this manuscript and approving it for publication was Jenny Mahoney.

section had the widest wheel trace distribution. It is evident that the measurement for only one single or a few sections wheel trace transverse distributions was not enough.

Wu [17] considered that the wheel trace transverse distributions were mainly determined by the standard deviation σ (the pilot takes the centerline of runway as its reference when taking off or landing, so the mean values should be concentrated near the centerline of runways and the range of the mean values is very small). During the takeoff process, the standard deviation σ is usually larger than at the runway ends. It is mainly because when an aircraft takes off, with increasing of the speed, it is more difficult for pilot to control the aircraft with equal precision. This leads to an increasingly large variance of wheel trace transverse distribution during the takeoff process. But during aircraft landings, the statistical trends are opposite to those seen for takeoff patterns. The literature assumed that the variation of wheel trace transverse distribution increases or decreases linearly with changes in the aircraft rolling speed. Based on that assumption, Wu derived the formula reflecting the rule of the wheels trace distribution along the runway. Nonetheless, [12] had considered that the trace trends did not simply increase or decrease, but may exhibited sideslip phenomenon in some areas and presented the theoretical algorithm for aircraft sideslip. Based on references [12], [13], [18] and statistical theory, a theoretical formula for runway width had been derived.

The above analyses on the rules for the wheel traces distribution still rested on theoretical assumptions. Until now, there is no test data to prove the accuracy of these analysis. It is also necessary to fully and accurately understand the variation of the wheel traces transverse distribution to ensure reliable runway width designs. In view of this problem, a multi-sections test system for wheel trace transverse distribution was designed in the paper. The on-site tests of wheel tracks were carried out at a feeder airport. The wheel traces transverse distributions and the variance rules of 17 cross sections were obtained based on the test results analysis. The maximum dispersion section of landing and the failure probability of 0.0001 % were selected to determine the runway width.

II. TEST PRINCIPLES AND TEST SYSTEM

A. TEST PRINCIPLES

Presently, wheel trace distribution test methods mainly consist of infrared telemetry, video method, the piezoelectric method, and laser telemetry [19]–[21]. These four methods all have their own advantages and disadvantages. Infrared telemetry uses a simple structure and has low cost [22]. However, it can easily be affected by the test environment, such as bird, high temperature of aircraft tail flame, et [23]. The video method is mainly used to measure the aircrafts wheel traces distribution. As an aircraft rolling speed is much larger than that of an automobile, this method has a remarkably high specifications requirement for a camera, which increases the system cost, which is not suitable for A large number of

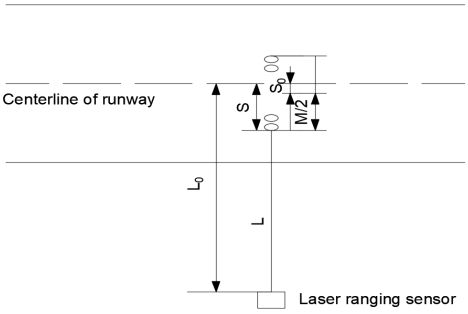

FIGURE 1. Measurement principle sketch.

lay [24]. The piezoelectric method has a low cost and high measurement accuracy, but has to bury the sensor beneath the runway pavement [25], which is hard to implement and maintenance. In comparison, laser telemetry has advantages of high maneuverability, high measurement accuracy, stability, and moderate costs [26]. Thus, the laser telemetry was adopted to carry out on-site tests for the work described in this paper.

When using laser telemetry to carry out tests for wheel traces transverse distributions, the measuring unit was placed on one side of the runway. The laser beam crosses the runway, perpendicular to runway centerline. When the aircraft wheels break the laser beam, the laser ranging unit measures the outer-side spacing between the aircraft main undercarriage outer wheel and the sensor (as shown in Fig. 1). According to Eq. (1), the distance from the outer-side space of outer wheels to the runway centerline can be calculated. Also, according to the configuration of aircraft undercarriage, the entire deviation of aircraft from runway centerline can be calculated by Eq. (2).

$$S = L_0 - L \tag{1}$$

$$S_0 = S - \frac{M}{2} \tag{2}$$

where L_0 denotes the distance between the laser sensor and the centerline of the runway, L denotes the measured value of the ranging unit, i.e., the distance between the sensor and the outermost side of main undercarriage outer wheel, S denotes the distance between the centerline of an aircraft wheel and the centerline of runway, M denotes the outer-side space of aircraft main undercarriage outer wheels, and S_0 denotes the deviation of aircraft entirety.

B. TEST SYSTEM

To test the wheel trace distributions of multiple sections, this system consists of seventeen groups of ranging units. All the ranging units were arranged along the runway length: they covered the main areas for aircraft takeoff and landing. Considering the larger ranging scope, the complicated environment of field tests and some uncertainty factors, the seventeen groups of ranging units were mutually independent from one another in order to avoid single damage affecting the whole tests and also to simplify the process of equipment

TABLE 1. Main technical parameters of test equipment.

Item	Standard range (Reflector)	Standard range (Rubber tire)	Measurement repetition accuracy	Measuring frequency	Power supply
Index	300m	200m	±5cm	2kHz-4kHz	DC 12V ± 20%, 5OOmA, ≤6W
Item	Volume	Operating temperature range (OTR)	Storage temperature range (STR)	Level of protection	Weight
Index	197×105 ×70 （mm）	-10°C—+50°C	-20°C—+70°C	IP66:IEC60529	1200g

installation. In this way, even if one group of test units broke down, it did not affect the normal operation of the other equipment.

The components of the test units contain a laser sensor, a storage unit, a mount and a power supply unit, as shown in Fig. 2. For the laser test sensor, the FSA-ITS02 laser ranging sensor was adopted, which is manufactured by Shenzhen Fashi Laser Radar Inc. Meanwhile, it has the functions to measure data and removing invalid data, with the technical parameters shown in Table 1. For the data storage unit, an industrial-grade serial port data recorder was adopted. It was manufactured by Shenzhen Jingmei Science & Technology Inc. It supports continuous recording at 921,600 bps and ensures that high-frequency measurement data from the laser ranging sensor are recorded. The mount is made of aluminum alloy. Without sacrificing the mount strength, the alloy dramatically reduces the mount weight and is convenient for transportation and installation. The length of mount can be adjusted in the range of 75 cm to 100 cm as required, and its pitch angle can be adjusted at the range of −45° to 45°. The power supply unit consists of a main battery and a standby battery. The main battery capacity is 60 Ah, which gives 60-hours normal operation. The standby battery capacity is 10 Ah, which is used for emergency conditions when main battery is depleted or damaged. It can power 10-hours normal operation.

a. Laser test sensor and storage cell

b. Mount

c. Power supply unit

FIGURE 2. Components of a single test unit.

C. INDOOR CALIBRATION

The indoor calibration of the laser test equipment should be carried out before the field test. The main purpose is to control the error between the laser indication point and the actual test point within a certain range, so that the equipment can be adjusted at the field test. In order to facilitate the installation of the testing system, the debugging board, shown in Fig.3, was made to simulate the main wheel of the aircraft. The height of the debugging board is designed to be 45cm to stipulate that the test area of the test laser beam must be in the lower half of the main wheel. At the same time, the lateral deviation between the test laser and the indicator laser should not be too large, and the width of the test plate is set to 30cm. In order to ensure that the test laser and the indicator laser are within the range of the debugging board (30cm×45cm) at the maximum possible test distance (about 100m), it is stipulated that the calibration error between the test laser and the indicator laser cannot exceed 4.5cm up and down during indoor calibration (about 10m). The left and right sides cannot exceed 1.5cm. The specific calibration steps are as follows:

FIGURE 3. Self-made device debug board.

1) Place the laser ranging test unit on a relatively flat desktop, and use a level measuring instrument to test whether the equipment is horizontal.

2) Use the debugging board to simply block the laser, and observe the change of distance display of the test unit.

3) When the bugging board is 10m away from the test unit. Move the debugging board to let the indicator laser fall at the midpoint of the calibration error line around. If the indicator laser falls on any calibration error line and the test unit has data display, the indicator precision of the laser indicator is qualified. Otherwise, the laser indicator shall be recalibrated according to the display result. For example, when the indicating laser falls on the calibration error line on the right, the test unit does not display, indicating that the laser indicator is on the left and should be adjusted to the right.

4) After the calibration of the test unit on one side is completed, take out the memory card to check the test data and verify whether the data processing unit and the data storage unit work normally.

The indoor debugging of the test system is shown in Fig. 4.

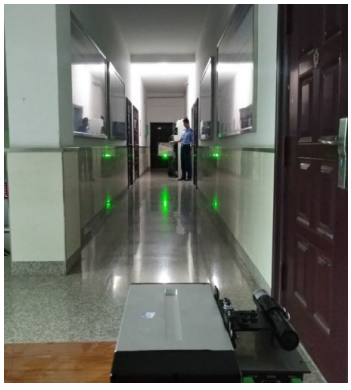

FIGURE 4. Indoor calibration diagram of test system.

III. OVERVIEW OF SITE TEST

A. TEST OF AIRPORT

A feeder airport in Northeast China was selected for the on-site test. The airport plan view is shown in Fig. 5. This airport is a 4C-level airport with a 2600 m×50 m runway. The basic aircraft type of the airport is the B737-300 and the single aircraft type is beneficial for more accurately studying the wheel trace transverse distribution. The schedules of 20 take-offs and landings are concentrated within the hours of 10:00 AM to 7:00 PM. The relatively dispersed flight time make the tester have plenty of time to install and maintain the devices, acquire data as well as change battery without affecting the flight.

B. DEVICE LAYOUT

The main takeoff/landing direction of the tested airport is north-south direction. Before taking off, the aircraft enters the runway from south linking taxiway along the taxiway, then enters the liftoff point, waiting for the takeoff order. Receiving the takeoff order, the aircraft will accelerate from liftoff point. For B737 aircraft, the distance traveled on the ground is 800-1100m under the normal full load (i.e., 85 % of the maximum take-off weight). During landing, aircraft uses the landing marking line as reference. The landing points are usually distributed within 200 m before or after the landing target mark. After landing, the aircraft decelerates, and rolls to a certain speed and keeps rolling at constant speed. At last, the aircraft taxis off the runway from north linking taxiway.

The laser ranging device was located at the flat area of south runway. The longitudinal layout distance was arranged according to the principle that half of the runway shall be covered, the landing site at the end of the runway and the takeoff site in the middle of the runway shall be densely arranged, and the taxiing region shall be appropriately sparse. As illustrated in Fig. 6, the test area is divided into three parts:

(1) Landing region: the initial position is 180m away from the end of the runway, and 8 instruments are installed in total, covering the landing area. (2) Middle taxiing region: a total of 3 sets of equipment are installed in the high-speed taxiing area; (3) Take-off region: a total of 6 instruments are installed to cover the take-off position of the test aircraft.

The distance from the instrument to the center line of runway meets the flight safety requirements, which is generally not less than 60m. In order to avoid the bird-riding vehicle passage and the other inconvenient installation area, the distance from the equipment to the runway center line ranges from 72m to 94m, with the specific values shown in Table 2.

C. DEVICE INSTALLATION

The device locations were determined according to the layout described in the above section. The mounts were embedded 25-30 cm into the ground. After the mount firmly set in the ground, the device was installed on the mount as shown in Fig. 7. The device was equipped with a special camouflage coat and waterproof bag to decrease its visibility and to provide self-protection in the field.

After a device was installed, the height and angle need to be adjusted to make sure the laser beam can irradiate the aircraft wheels. The adjustments were conducted as seen in Fig. 8

FIGURE 5. Test airport plan view.

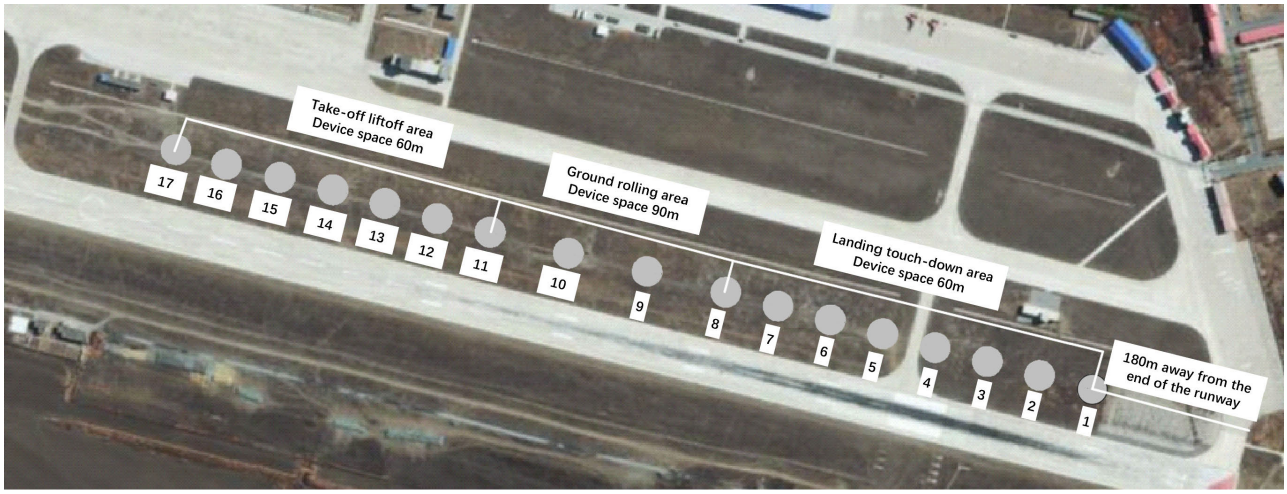

FIGURE 6. Device layout.

TABLE 2. The distance between unit and the runway centerline.

Device number	1	2	3	4	5	6
Distance (m)	72.2	73.5	78.2	78.6	82.7	82.9
Device number	7	8	9	10	11	12
Distance (m)	83.1	87.8	63.2	87.8	88.8	88.5
Device number	13	14	15	16	17	
Distance (m)	89.01	90.9	91.3	92.2	93.3	

1) Use an electronic inclination meter to adjust pitch angle of the device to keep the device horizontal during the measurement process as shown in Fig. 8a.

FIGURE 7. Installed device.

2) a tester stands near the runway centerline and the test board is set on the runway and perpendicular to the laser beam direction. Another tester adjusts the height of the mount and its left to right drift angle, making the beam of the visible laser indicator in leaser sensor stay on the reference point in the test board. In this way, the device height and the rough measurement direction of device is determined.

a. Adjust the device angle of pitch

b. Vertical adjustment of device

FIGURE 8. Adjustment of device.

3) As shown in Fig.8b, one tester moves the test board within a small range around the runway centerline. At the same time, the other tester adjusts the mount left and right to make the beam of the visible laser indicator stay on the reference point of the test board and observe the angle displayed on laser sensor. When the angle reaches a minimum value, the measuring laser is parallel to the runway.

D. ANALYSIS OF TEST ERRORS

There are two main aspects of the test errors. One aspect is the error caused by the slope of the runway, as shown in Fig. 9. The result obtained from Eq. (1) is the straight-line distance between the centerline of an aircraft wheel and the runway centerline. However, we need the transverse distance along the runway between the aircraft wheels centerline and the runway centerline. Due to the runway slope, there is a certain difference between those two distances. The distance should therefore be converted and calculated according to Eq. (3). Before the test, it is necessary to carry out measurements for the runway slope of each test section (Fig. 10). The results are shown in Table 3. The second source of the error is caused by the test environment, including the moving vegetation, low-flying birds, et., which may lead to invalid data because of the laser reflection off these objects. This problem can be solved by setting the sensor parameters, as shown in Fig. 9. On one hand, the measurement range of the sensor can be limited to a certain range. For example, sensor No.1

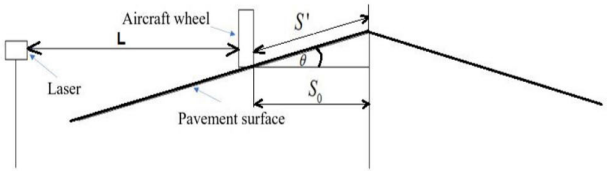

FIGURE 9. Slope error diagram.

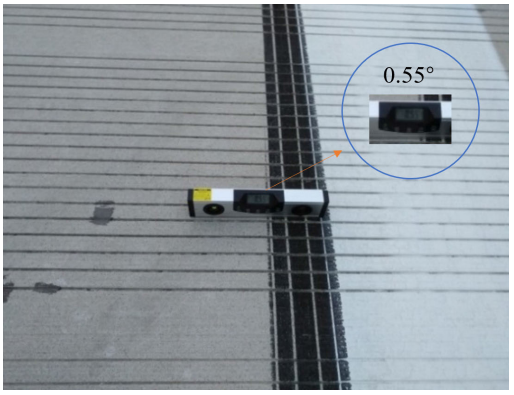

FIGURE 10. Measurements of runway slope.

is 72.2 m away from the runway centerline and the runway width is 50 m, so the measurement range of sensor No. 1 is set to 45 to 90 m. On the other hand, the data record threshold of sensor is also can been set. Since the acquisition frequency of the sensor data is 2 kHz, the aircraft takeoff and landing speed is 80 m/s and the main wheel diameter of B737 is about 0.97 m, the sensor can collect at least 25 datapoints as an aircraft wheel passes the measurement laser. The number of datapoints acquired is hard to achieve with the moving vegetation or low-flying birds. Therefore, the system can be set so that the sensor begins to record an object distance only after collecting 25 datapoints. If the number of datapoints is less than 25, the corresponding distance values can be regarded as an invalid data.

$$S' = \frac{S_0}{COS\theta} \tag{3}$$

where S' denotes the transverse distance between aircraft and the runway centerline, and the angle of inclination θ denotes the runway slope.

IV. ANALYSIS OF STATISTICAL RULES FOR THE WHEEL TRACES TRANSVERSE DISTRIBUTION

A. STATISTICAL RULES FOR WHEEL TRACES TRANVERSE DISTRIBUTION DURING TAKEOFF

First, whether a single-section wheel trace transverse distribution follows a Gaussian distribution was verified, since almost all current studies took that point of view. Normal assumptions were conducted for the wheel trace transverse distributions when a B737-300 aircraft takes off, for the 17 test sections along the runway. The mean and variance were calculated. The K-S test (level of significance: 0.05) was

FIGURE 11. Setting the sensor parameters.

TABLE 3. Normal distribution fitting data for each cross section of aircraft takeoff.

Device number	Parameter estimation		K-S test
	μ	σ	p values
1	0.09	0.99	0.275
2	0.05	1.04	0.376
3	-0.02	1.08	0.277
4	-0.11	1.19	0.563
5	-0.04	1.25	0.380
6	0.11	1.39	0.754
7	0.15	1.45	0.685
8	0.04	1.78	0.0887
9	0.16	2.02	0.115
10	0.17	2.21	0.0988
11	-0.13	2.48	0.145
12	0.02	2.32	0.545
13	0.18	2.55	0.987
14	0.22	2.56	0.124
15	0.16	2.64	0.0954
16	-0.09	2.59	0.354
17	0.21	2.67	0.456

used to verify the normal assumption is true or false. The specific values are shown in Table 3. The Cartesian coordinate system was setup at the mid-point of the runway edge. The lateral edge of the runway is in x-direction, and the center line of the pavement is y-axis. The aircraft deviation to one side of device is recorded as positive deviation, and to the other side of device is recorded as negative deviation. It can be seen from Table 4 that all the p values of sections of the K-S test are larger than required for a 0.05 level of significance. This indicates that it is a high probability event that the wheel traces transverse distributions on the 17 sections follow a

TABLE 4. Normal distribution fitting data for each cross section of aircraft landing.

Device number	Parameter estimation		K-S test
	μ	σ	p values
1	0.18	3.08	0.655
2	0.05	3.25	0.235
3	-0.09	3.59	0.0956
4	-0.21	3.65	0.284
5	-0.24	3.89	0.987
6	-0.08	3.78	0.754
7	0.15	3.25	0.0951
8	-0.04	3.18	0.0924
9	0.16	2.49	0.754
10	0.17	2.51	0.354
11	-0.13	1.68	0.456
12	0.02	1.88	0.0987
13	0.18	1.48	0.784
14	0.22	1.24	0.245
15	0.16	1.35	0.645
16	-0.09	1.25	0.0854
17	0.21	1.17	0.459

Gaussian distribution, as assumed in prior work such as [27]. However, the mean and variance of a Gaussian distribution on every section are different, so further analysis is needed to calculate the statistics for the variation of the wheel traces transverse distributions along the length of the runway.

Fig. 12 shows the relationship between mean and variance of each section wheel trace transverse distribution for each section, during the takeoff runs of the B737-300. It can be seen from the figure that the variation of the mean of the wheel traces transverse distributions for every section is centered very close to the runway centerline, and the deviation is small. The measured values indicate that the largest deviation when taking off is 4.8 m, while the largest deviation from the mean is 0.21 m, less than 5 % of the aircraft largest deviation. The minimum value is 0.09 m. For convenient calculation, it can be similarly considered that the mean of each section wheel trace transverse distribution is 0 as aircraft takes off. However, the variation is large, with the minimum value of 0.99 and the maximum value of 2.67. With the increase of the aircraft rolling distance on the ground, the rolling speed also increases, and the variance of wheel trace transverse distribution also increases. However, the trend of variance increasing with distance is not linear. With the increase in the rolling distance, the change of the aircrafts ground speed with the same rolling distance is small, but the change of variance is larger. Until it reaches the liftoff area when the rolling speed

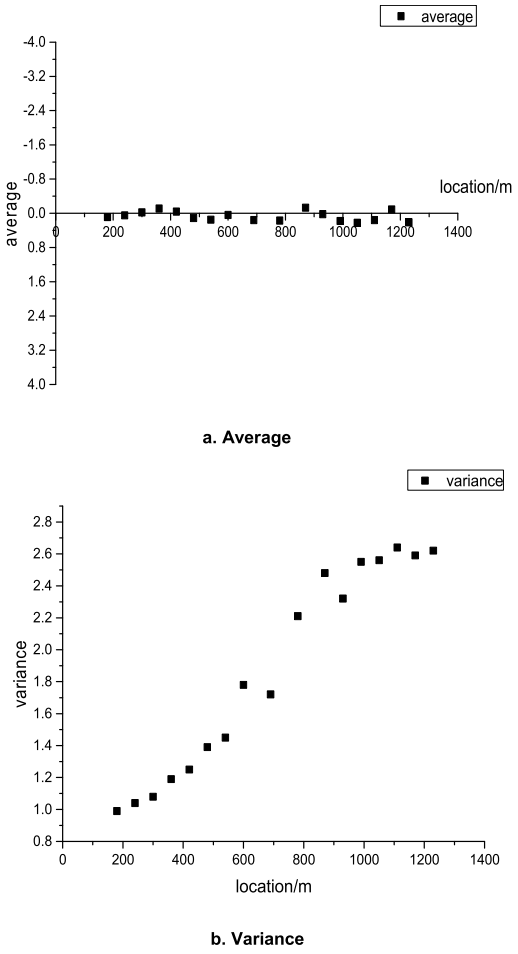

FIGURE 12. Relationship between each section wheel trace transverse distribution average and variance with the runway location where the section is (takeoff).

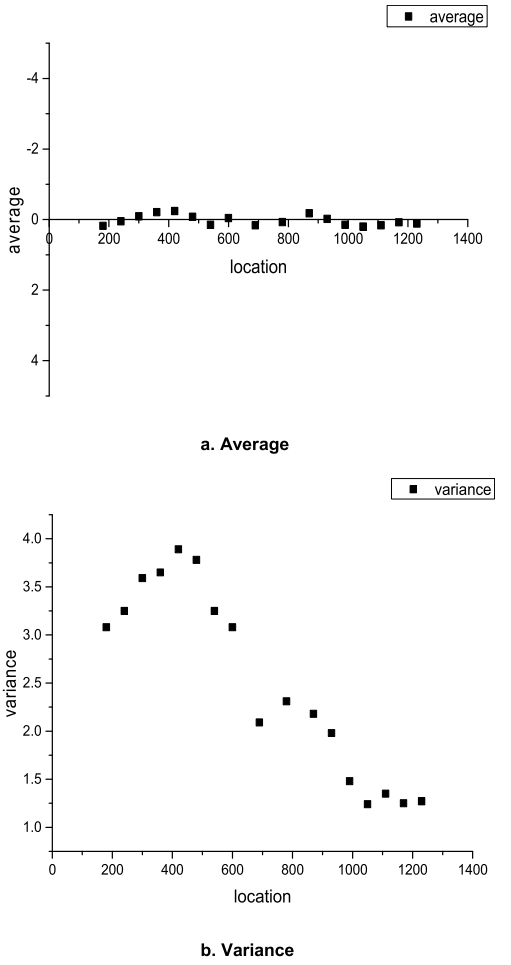

FIGURE 13. Relationship between each section wheel trace transverse distribution average and variance with the runway location where the section is (landing).

reaches its maximum value, the change of variance tends to be smooth.

B. STATISTIC RULE FOR WHEEL TRACES TRANSVERSE DISTRIBUTION DURING AIRCRAFT LANDING

Table 4 shows the normal assumption test results for each section wheel trace transverse distribution during landing. It shows that the p values by K-S test of all the runway sections are all larger than needed for the 0.05 level of significance: each section wheel trace distribution of B737-300 aircraft when landing follows the Gaussian distribution. Also, it shows that the varied degree of transverse distributions in landing is more intense than that in takeoff, with the largest variance reaching 3.89. This contrast shows it is more difficult to control the direction of aircraft during landings than during takeoff.

Fig. 13 shows the relationship between the mean and variance of each section wheel trace transverse distribution when aircraft land and the runway location of that section. It can be seen from the figure that when a B737-300 aircraft lands, the variation in the mean of each section wheel trace transverse distribution also concentrates around the runway centerline. Although the degree of variation is larger than what is seen in data from takeoffs, with a maximum value reaching to 0.24 m, the aircraft deviation during landing increases after touchdown, with the maximum deviation reaching 5.2 m. The variation in mean is still 5 % less than the maximum deviation. During the calculation, the mean of each section wheel trace transverse distribution is close to zero as well. Therefore, the assumption about the variation in mean of wheel trace transverse distribution in [14] is feasible. During landing, the variance is very different from what is seen during takeoff. In the aircraft touch-down area, the variance of the wheel traces transverse distributions has a significant increasing trend after touchdown. But the duration of this increasing trend is very short. In a range of 400-450 m away from the runway touchdown end, the variance reaches its maximum value, and then the variance starts to decrease sharply. As the aircraft ground rolling distance after touchdown increases, its rolling speed decreases and the variance changes tend to be smooth. It indicates that in a short period after landing, an aircraft indeed often experiences sideslip to

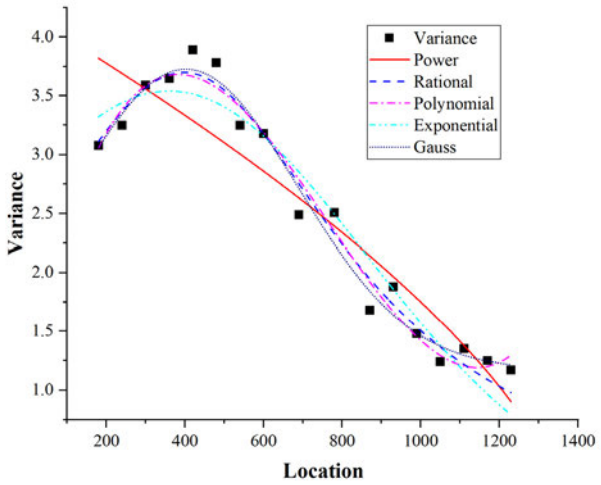

FIGURE 14. The fitting results (landing).

a certain extent, but it is quickly controlled by the pilot and gradually draws close to the runway centerline, which verifies the assumption in [15].

V. RUNWAY WIDTH DESIGN

A. DETERMINATION OF THE SECTION WITH LARGEST DISPERSION

It is known from the above analysis that the discretization of wheel traces transverse distributions in landing is larger than taking-off. Therefore, during the design of runways widths, the statistical variation of the wheel traces transverse distribution in landings should be considered. The extent of the discretization of wheel traces distributions is mainly determined by variance. In order to calculate the largest variance of the wheel traces transverse distributions for aircraft landings, the expression of the variation rule during landings is obtained through curve fitting. The maximum value of the expression in the landing rolling range is found.

To make the fitting result more accurate, five frequently-used curve model (i.e., Rational, Power, Polynomial, Gauss and Exponential) were fitted to the test results. The curve model with the best fit was selected to be the final result. The fitting results are shown in Fig. 14, indicating the Power model has an obviously poorer fit and can be ignored. The other four model can model the variation rule of the landing process statistical variance of landing to a good degree. It cannot be seen which model is better only from that figure, so further mathematical analysis of the curve fit results is needed.

In order to compare the four models, two kinds of evaluation criterion are introduced: SSE and R-squared [28]. SSE denotes the quadratic sum of the errors between the fitted data and the corresponding points of the original data. The more closely SSE approaches 0, the closer to the original data the fitted data are. The R-square approach denotes the ratio between the quadratic sum of the differences between the predicted data and the mean of the original data (SSR), and, the quadratic sum of the difference between the original data and that original data mean (SST). The more closely it approaches 1, the stronger the ability of that predictive model results will be when compared to measured data. It also indicates that this model fitting effect is better. The mathematical analysis results for the curve fitting results are shown in Table 5. It shows that for either SSE or R-squared approaches, the Rational model has the best fitting results. Hence, the expression for the wheel traces transverse distribution variance during landing is shown in (4), in which the maximum value in the ground rolling range is 3.81 m, and then the expression of the section with the largest dispersion degree of wheel trace distribution is $S' \sim N(0, 3.81)$.

TABLE 5. The mathematical analysis results for the curve fitting results.

	Polynomial	Gauss	Exponential	Rational
SSE	0.795586	1.165169	0.759451	0.560184
R-square	0.936741	0.89051	0.939614	0.951747

TABLE 6. The failure probabilities corresponding to different runway widths.

Runway width	41	42	43
Failure probabilities	7.14E-06	3.82E-06	2.01E-06
Runway width	44	45	46
Failure probabilities	1.04E-06	5.32E-07	2.67E-07

$$y = \frac{0.737x^2 - 514.6x + 570400}{x^2 - 764.3x + 272900} \tag{4}$$

where y denotes the variation of the wheel traces transverse distribution, and x denotes the location of the corresponding section of the runway.

B. RUNWAY WIDTH VALUES

To ensure the safety of aircraft rolling on a runway, the probability of an aircraft rolling off the runway (failure probability) should be well controlled with an extremely small range. Reference [18] analyzed this question and concluded the accidents of aircraft rolling off the runway as well as the accident-proneness of China military and civil aviation during recent ten years. That research found that, apart from the accidents caused by mechanical breakdown, the average failure probability of aircraft running out of runway is 4.139×10^{-6}. To improve the safety standard, here the failure probability is taken as 0.0001 %. The outside spacing between B737-300 aircraft main wheel felly is 6.79 m, the runway design width is W, so $P(S' > \left|\frac{W-6.79}{2}\right|)$ should be less than 0.0001 %. Table 6 lists the failure probabilities corresponding to different runway widths. It shows that B737-30 should have at least 45 m width to ensure the probability of failure being 0.0001 %.

VI. CONCLUSION

In this paper, a new runway width design method was proposed based on the wheel traces distribution of aircrafts. A laser test system was developed to measure the aircraft wheel tracks of 17 cross sections along the runway at a feeder airport. Following conclusion can be drawn from the test results:

1) When the aircraft takes off, the wheel traces follow a Gaussian distribution, with the mean values approximately to 0. With increasing of rolling distance, the aircraft rolling speed also increases, and wheel traces transverse distribution increases with an obvious trend until the aircraft reach the liftoff area.

2) When the aircraft lands, the wheel traces also follow a normal distribution, with the mean values approximately to 0. The changes of variance are greater than those seen when the aircraft takes off. In the touch-down area of a runway, the wheel traces transverse distribution has an obvious increasing trend. However, the increasing trend only lasts for a short time. In the runway section 400-450 m, the variance reaches its maximum and then begins to decrease. With the increase of aircraft rolling distances, the rolling speed decreases and the change in variance tends to be smooth.

3) The statistical rule for the variance of the wheel traces distribution when landing can be well modeled by Rational model. Through curve fit results, the maximum variance in the rolling section of a runway is 3.81 m.

4) For B737-300 aircraft, a runway with a width at least 45m is needed to ensure the failure probability of being 0.0001 %.

CONFLICT OF INTEREST

The author declares no conflict of interest regarding the publication of this paper.

REFERENCES

[1] *Managing Airports 4th Edition*, Graham, Batavia, NY, USA, 2013.
[2] F. Scholz, "Statistical extreme value analysis of ANC taxiway centerline deviations for 747 aircraft," FAA, Washington, DC, USA, Tech. Rep. 20591, 2003.
[3] F. Scholz, "Statistical extreme value analysis of JFK taxiway centerline deviations for 747 aircraft," FAA, Washington, DC, USA, Tech. Rep. 20592, 2003.
[4] F. Scholz, "Statistical extreme value analysis concerning risk of wingtip to wingtip or fixed object collision for taxiing large aircraft," Tech. Rep., 2005.
[5] D. Cohen-Nir and R. Marchi, "Preliminary analysis of taxiway deviation data and estimates of airplane wingtip collision probability," *Transp. Res. Rec., J. Transp. Res. Board*, vol. 1850, no. 1, pp. 49–60, Jan. 2003.
[6] *International Civil Aviation Organization*, Aerodrome Design and Operation, Aerodromes, Kerala, 2004.
[7] *APSDS 4 User Manual Airport Pavement Structural Design System*, MINCAD Systems, Richmond, Australia, 2000.
[8] *Guideline on PCN Assignment in The Netherlands*, CROW, Amsterdam, The Netherlands, 2005.
[9] Z. H. Wang, L. C. Cai, and Q. K. Gu, "Airport rigid pavement cumulative damage optimization model considering load stress distribution," *China Civil Eng. J.*, vol. 11, pp. 143–150, Jan. 2011.
[10] L. Li, "Reliability design of military runway plane size," Ph.D. dissertation, Air Force Eng. Univ., Xi'an, China, 2009.
[11] *Chinese Specifications for Asphalt Pavement Design of Civil Airports: MH/T 5010-2017*, Civil Aviation Administration, China, Beijing, 2017.
[12] G. Y. Li, "Course stability of aircraft on double-sided cross slope runway," *J. Transp. Eng.*, vol. 2, no. 3, pp. 112–114, 2002.
[13] G. P. Cen, S. Lu, and G. Hong, "Research on reliability design method of runway width," *Sci. Technol. Guide*, vol. 32, no. 22, pp. 47–51, 2014.
[14] A. V. Hosang, "Field survey and analysis of aircraft distribution on airport pavements," Transp. Res. Board, Washington, DC, USA, Tech. Rep. FAA-RD-74-36, 1975.
[15] E. H. Guo, G. F. Hayhoe, and D. R. Brill, "Analysis of NAPTF traffic test data for the first-year rigid pavement test items," in *Ederal Aviation Administration Technology Transfer Conference*, Atlantic City, NJ, USA: ASCE, May 2002.
[16] J. Yuan, E. H. Shi, and D. Lei, "Lateral deviation pattern and model of aircraft wheel path on Shanghai Hongqiao international airport," *J. Civil Aviation Univ. China*, vol. 4, pp. 1–6, May 2015.
[17] A. H. Wu, *Studies on the Design Method of Airport Pavement Based on Cumulative Damaged Curved Surface*. Xi'an, China: Air Force Engineering Univ., 2012.
[18] S. Lu, *Reliability Research of Military Airport Flight Area Plane Size*. Xi'an, China: Air Force Engineering Univ., 2014.
[19] W. Gawron, Z. Bielecki, and J. Wojtas, "Infrared detection module for optoelectronic sensors," *Proc. SPIE Infr. Technol. Appl.*, vol. 8353, May 2012, Art. no. 83532U.
[20] Y. Fang, W. Lin, Z. Chen, C.-M. Tsai, and C.-W. Lin, "A video saliency detection model in compressed domain," *IEEE Trans. Circuits Syst. Video Technol.*, vol. 24, no. 1, pp. 27–38, Jan. 2014.
[21] D. D. Pham and Y. S. Suh, "Remote length measurement system using a single point laser distance sensor and an inertial measurement unit," *Comput. Standards Interface*, vol. 50, pp. 153–159, Feb. 2017.
[22] Y. Chen, Z. Meng, J. Liu, and H. Jiang, "High-precision infrared pulse laser ranging for active vehicle anti-collision application," in *Proc. Int. Conf. Electr. Inf. Control Eng.*, Apr. 2011, pp. 1404–1407.
[23] J. Yuyi, L. Keshen, and R. Yanghui, "Wheeled maze robot design based on ranging infrared sensor," *Microcontrollers Embedded Syst.*, vol. 9, p. 22, Jun. 2013.
[24] H. Z. Ma, "Design and research of vehicle flow detection system based on video image processing technology," *J. Changchun Univ. Eng.*, vol. 16, no. 4, pp. 109–112, 2015.
[25] G. Loprencipe and P. Zoccali, "Comparison of methods for evaluating airport pavement roughness," *Int. J. Pavement Eng.*, vol. 20, no. 7, pp. 782–791, Jul. 2019.
[26] T. Bosch, "Laser ranging: A critical review of usual techniques for distance measurement," *Opt. Eng.*, vol. 40, no. 1, p. 10, Jan. 2001.
[27] G. F. Barrett, S. G. Donald, and D. Bhattacharya, "Consistent nonparametric tests for lorenz dominance," *J. Bus. Econ. Statist.*, vol. 32, no. 1, pp. 1–13, Jan. 2014.
[28] R. Bramante, G. Petrella, and D. Zappa, "On the use of the market model R-square as a measure of stock price efficiency," *Rev. Quant. Finance Accounting*, vol. 44, no. 2, pp. 379–391, Feb. 2015.

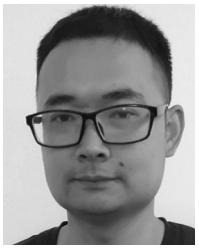

DUOYAO ZHANG received the B.S., M.S., and Ph.D. degrees in airport engineering from Air Force Engineering University, Xi'an, China, in 2012, 2015, and 2019, respectively.

His research interests include airport pavement design and evaluation and pavement materials.

XINGANG SHI received the B.S. and M.S. degrees in airport engineering from Air Force Engineering University, Xi'an, China, in 2014 and 2016, respectively, where he is currently pursuing the Ph.D. degree in airport engineering.

His research interests include planning and management of airport, airport pavement design and evaluation, pavement materials, and mechanical simulation of aircraft.

LIANGCAI CAI received the B.S. and M.S. degrees in airport engineering from Air Force Engineering University, Xi'an, China, in 1984 and 1987, respectively, and the Ph.D. degree in road and railway engineering from Southeast University, in 1995. He is currently a Professor with the Department of Airport Engineering and Architecture, Air Force Engineering University.

His research interests include planning and management of airport, environmental protection and evaluation of airport, and airport pavement design.

GUANHU WANG received the B.S., M.S., and Ph.D. degrees from Air Force Engineering University, in 2002, 2005, and 2009, respectively. He is currently an Associate Professor with the Department of Airport Engineering and Architecture, Air Force Engineering University.

His research interests include planning and management of airport.

CHAOMEI MENG, photograph and biography not available at the time of publication.

LEI LIANG, photograph and biography not available at the time of publication.